Global Change Biology

Global Change Biology (2009) 15, 3056–3065, doi: 10.1111/j.1365-2486.2009.01936.x

When to worry about the weather: role of tidal cycle in determining patterns of risk in intertidal ecosystems

K. A. S. MISLAN, DAVID S. WETHEY and BRIAN HELMUTH

Department of Biological Sciences, University of South Carolina, 715 Sumter Street, Columbia, SC 29208, USA

Abstract

Species range boundaries are determined by a variety of factors of which climate is one of the most influential. As a result, climate change is expected to have a profound effect on organisms and ecosystems. However, the impacts of weather and climate are frequently modified by multiple nonclimatic factors. Therefore, the role of these non-climatic factors needs to be examined in order to understand and predict future change. Marine intertidal ecosystems are exposed to heat extremes during warm, sunny, midday low tides. Thus, the timing of low tide, a nonclimatic factor, determines the potential contact intertidal invertebrates and algae have with heat extremes. We developed a method that quantifies the daily risk of high temperature extremes in the marine intertidal using solar elevations and spatially continuous tidal predictions. The frequency of 'risky days' is variable over time and space along the Pacific Coast of North America. Results show that at some sites the percentage of risky days in June can vary by 30% across years. In order to do a detailed analysis, we selected San Francisco as a study site. In San Francisco, May is the month with the greatest frequency of risky days, even though September is the month with the greatest frequency of high air temperature, $\geq 30\,^{\circ}$C. These results indicate that marine intertidal organisms can be protected from high temperature extremes due to the timing of tides and local weather patterns. In addition, annual fluctuations in tides influence the frequency of intertidal zone exposures to high temperature extremes. Peaks in risk for heat extremes in the intertidal zone occur every 18 years, the length of the tidal epoch. These results suggest that nonclimatic variables can complicate predictions of shifts in species ranges due to climate change, but that mechanistic approaches can be used to produce predictions that include these factors.

Keywords: biogeography, boundary, climatology, ecological forecasting, El Niño, littoral, Pacific Decadal Oscillation, range

Received 10 November 2008; revised version received 27 February 2009 and accepted 3 March 2009

Introduction

Geographic distributions of species are well-known to respond to temperature (Hutchins, 1947; Darlington, 1957; Lewis, 1964; MacArthur, 1972); so, increases in temperature associated with climate change were expected to significantly affect range distributions (IPCC, 2007) as has now been documented across very different ecosystems (Helmuth *et al*., 2006b; Lima *et al*., 2006, 2007; Parmesan, 2006; Moritz *et al*., 2008). However, species distributions and patterns of abundance are often not simple correlates of trends in surface, water, and air temperature because of small-scale habitat characteristics, physical interactions of organisms with their habitats, behavioral and physiological adaptations, and habitat degradation and loss (Burrows & Hughes, 1989; Huey *et al*., 1989; Sala *et al*., 2000; Bonan, 2002; Helmuth *et al*., 2002; Holtmeier & Broll, 2005; Franco *et al*., 2006; Kearney, 2006; Moore *et al*., 2007; Poloczanska *et al*., 2008). In addition, the influences of surface, water, and air temperature are complicated by nuances in instantaneous weather conditions and long-term climate trends which are often temporally non-linear and/or spatially heterogeneous (Mantua *et al*., 1997; Mantua & Hare, 2002; IPCC, 2007; Kenyon & Hegerl, 2008). One such complication is that weather variables other than temperature, such as wind and

Correspondence: K. A. S. Mislan, tel. + 803 777 3931, fax + 803 777 4002, e-mail: kas.mislan@gmail.com

precipitation, also affect species range boundaries both as modulators of temperature and independently (Helmuth, 1998; Körner, 1998; Wethey, 2002; Davies & Johnson, 2006; Gilman *et al*., 2006b; Helmuth *et al*., 2006a). Additionally, extreme weather events can exert effects on organisms via 'threshold' effects (Wethey, 1985; Wethey, 1986; Easterling *et al*., 2000) so changes in species distributions may occur suddenly.

Given these complexities, the use of models based on weather and climate data as key tools to determine the most influential biological and physical factors is expanding. There are two main classes of models used for this purpose, bioclimatic envelope models and mechanistic models. Bioclimatic envelope models use correlations between environmental variables and geographic distributions to determine the relative strength of an individual environmental variable on an organism (Pearson & Dawson, 2003; Thuiller, 2003). Mechanistic, also called process-based, models isolate and characterize the most important environmental variables for a particular species by using physical models of heat exchange in combination with physiological and ecological studies (Wethey, 1986, 2002; Morin *et al*., 2007, 2008; Poloczanska *et al*., 2008; Wethey & Woodin, 2008). Information derived from both of these types of models using past conditions can be used to make future predictions (Pearson & Dawson, 2003; Araújo *et al*., 2005; Helmuth *et al*., 2006b; Pearson *et al*., 2006). Since climate change is of utmost concern, scientists primarily focus on the role climate change will have on future biogeographic ranges when making predictions (Davis *et al*., 1998; Sutherst *et al*., 2007). However, nonclimatic factors may be key drivers of species range boundaries and patterns of physiological stress (Denny & Paine, 1998; Sala *et al*., 2000; Helmuth *et al*., 2006b) or, alternatively, may enhance or lessen the impact of changes in climate (Porter *et al*., 2002; Hsieh *et al*., 2008). Nonclimatic factors are aspects of the environment not directly related to climate (geographical features, biological interactions, and anthropogenic effects) that impact an organism and should be investigated simultaneously with climatic factors in order to prevent overestimates or underestimates of changes in biogeographic ranges of species that are influenced by nonclimatic factors.

The marine intertidal zone is an environment where nonclimatic factors are influential because intertidal organisms are only vulnerable to weather during aerial exposure at low tide. Tides, a nonclimatic variable, are daily changes in ocean height due to the movements of the sun and moon in relation to the earth. Sedentary intertidal organisms that live along the land–ocean interface are submerged by ocean water during high tide and subsequently emersed into the terrestrial environment during low tide once or twice per day. Intertidal organisms, which are ectotherms of marine origin, have body temperatures driven by water temperature when submerged during high tide and by local weather conditions when emersed during low tide. Body temperature extremes can be fatal to intertidal organisms and usually occur during low tide – high temperature extremes occur during mid-day low tides, and cold temperature extremes occur during predawn low tides (Bell, 1995; Helmuth *et al*., 2002).

Denny & Paine (1998) emphasized the need to consider long-term trends in tide by demonstrating the effect of the 18.6-year lunar cycle. They found cyclical trends in both water temperature and daytime emersion times associated with tides and were able to tie these long-term trends to variability in intertidal communities. Spatial variation in tidal cycle has also been analyzed, and the timing and duration of low tide was found differ between sites on the same coastline (Helmuth *et al*., 2002; Finke *et al*., 2007). Along the West Coast of North America, Helmuth *et al*. (2002, 2006a) linked spatial variation in mid-day emersion to patterns of body temperature in intertidal mussels by showing that mussel body temperatures were higher at sites with more mid-day emersion during summer months even though the sites with more mid-day emersion were farther from the equator. This demonstrates that spatial variability in the timing of low tides, a nonclimatic factor, can override large-scale patterns of climate that occur between the equator and poles (Helmuth *et al*., 2006a, b).

Tides are a nonclimatic factor that may interfere with the response of the intertidal community to long-term changes in climate by decreasing the frequency of exposure to harmful weather conditions. In this study, we refer to tidally controlled contact with weather conditions as 'risk.' We determine risk for intertidal organisms by using tidal predictions and solar movements to estimate exposure to direct solar radiation during 'low tides when the sun is high in the sky.' This risk metric was selected because exposure to direct solar radiation, which in this case is partly controlled by tides, is the major determinant of harmful body temperatures (Helmuth, 1998; Wethey, 2002; Denny & Harley, 2006; Gilman *et al*., 2006b; Burnaford & Vasquez, 2008). We developed a latitudinally adapted analysis that uses solar elevations and spatially continuous tidal predictions. This is a critical improvement over previous studies which used a metric of risk based on total hours of mid-day exposure (11:00–13:00 hours) that was not adjusted for latitude or sun elevation, and which were restricted to sites with tide stations (Helmuth *et al*., 2002; Finke *et al*., 2007). Moreover, we explore whether a higher probability of risk leads to a greater frequency of high temperature exposures and vice versa. Our intent is to examine the role of tidal cycles in driving past, present, and future climate change risk in the intertidal zone and provide a projection of the relative role of the tidal cycle in determining the susceptibility of intertidal ecosystems to increasing warming. Although this method can easily be employed on a worldwide basis, we focus on the West Coast of North America because it is a well-studied marine intertidal region (Ricketts & Calvin, 1939; Light *et al.*, 1954; Schoch *et al.*, 2006; Blanchette *et al.*, 2008; Broitman *et al.*, 2008).

Data and methods

Tidal predictions were obtained using the Oregon State University (OSU) Tidal Prediction Software (OTPS) with the OSU Tidal Inversion Software (OTIS) regional model of the West Coast of North America (Egbert *et al.*, 1994; Egbert & Erofeeva, 2002), and solar elevations were obtained from the NASA Jet Propulsion Laboratory Horizons Ephemeris System (Giorgini *et al.*, 1996). These data were used to estimate hourly exposure to direct solar radiation during 'low tides when the sun is high in the sky.' A high risk day was identified when the following inequality was true for more than 2 hours on a particular day.

$$(h - f(t))\cos(90 - g(t)) \cdot s > 0$$

In this formula, h is the shore level (of the organism or species boundary of interest) in meters above the reference datum; $f(t)$ is the tide height at time t in meters above the reference datum; $g(t)$ is the sun elevation in degrees at time t; and s is solar radiation on a clear day in W/m^2. The term $[h-f(t)]$ is inversely related to the probability of cooling of the shore at height h by wave splash. Thus, when $f(t)$ is close to h, the risk of wave splash is high and the risk of exposure to extreme terrestrial conditions is low. Note that for the comparative purposes examined here, wave height is considered to be a constant term, although the inclusion of wave splash in future applications of the equation may be possible (Harley & Helmuth, 2003; Gilman *et al.*, 2006a). The term $[\cos(90-g(t))]$ modifies the intensity of direct solar radiation on a horizontal surface as a function of the angle of incidence to indicate time of day. The highest values of $[\cos(90-g(t))]$ are at local solar noon when the sun is highest in the sky and exposure to heat extremes is most likely. Solar radiation, s, is set at a constant value because this analysis is designed to look at variation in tides, a nonclimatic variable. The units of the inequality are W/m. Positive values indicate that the intertidal community is potentially exposed to thermally stressful conditions because the low tide occurs at a time of day when the sun is high in the sky. We will refer to 2 + hours per day of positive values as 'risky conditions' throughout the rest of this paper.

Specific parameters were selected for the risk analysis. The shore level h was set at geoid sea level which is approximately the midpoint of the tidal range (Robinson, 2004). Wave surge, on average, increases the still tide height approximately 0.30 m during summer months along this coastline so h was adjusted to be 0.30 m below geoid sea level (unpublished data). A regional tide model was used because it provided accurate water level predictions at a latitudinal resolution of 0.083° for shallow coastal waters. It included the tidal constituents: m2, s2, k1, o1, n2, k2, p1, q1 (Egbert & Erofeeva, 2002). Only solar elevations, $g(t)$, $> 50^{\circ}$ were considered risky. Solar radiation on a clear day, s, was approximated as a constant $1000\ W\ m^{-2}$. We considered a day to be 'high risk' when the risky conditions occurred for more than 2 h. A time threshold was necessary because it takes time for intertidal organisms to heat up to harmful body temperatures from sea surface temperature, the initial temperature of intertidal organisms when first exposed by the tides (Helmuth, 1999; Wethey, 2002; Denny *et al.*, 2006; Gilman *et al.*, 2006b). However, while we generically chose 2 h as a threshold, it is important to note that heating rate will vary according to size and morphology of individual organisms (Helmuth, 1999). Risk is presented as a probability, with number of days with high risk divided by total days, to reflect the fact that it is only a possibility that intertidal ecosystem will be exposed to high temperatures on a particular day. It is important to note that this risk model is based on a cloud-free and fog-free environment, and serves as a baseline from which to measure risk due to mid-day low tide in the absence of other mitigating factors. To the extent that these factors vary seasonally and geographically, the actual risk to intertidal organisms may differ from model predictions.

We selected San Francisco, which has continuous long-term air temperature data, as an example study site to determine if long-term tidal variation can lead to temporal variation in exposure to high air temperatures. Air temperature was selected as a comparative weather variable because there are extensive historical records. Air temperature is not always equal to ectotherm body temperature during low tide, and ectotherm body temperatures can vary greatly based on size, color, and morphology of individual organisms (Southward, 1958; Porter & Gates, 1969; Etter, 1998; Helmuth, 1998; Denny *et al.*, 2006; Szathmary *et al.*, 2009). However, many of the same weather factors including solar radiation, wind speed, and humidity that determine air temperature also determine ectotherm body temperature during low tide. Therefore, maximum daily air temperature was used as a measure of general terrestrial weather conditions. Our assumption was that ectotherm body temperatures during low tide on days when the sun is high in the sky were generally higher on days with higher air temperatures (Denny *et al*., 2006).

Maximum daily air temperatures for the San Francisco International Airport (COOPID: 047769, WBANID: 23234, latitude: 37.617N, longitude: 122.400W) were obtained from the National Climatic Data Center (NCDC). These temperatures were compared with risk data from corresponding outer coast coordinates (37.665N, 122.500W). Maximum daily air temperatures of $\geq 30\,^{\circ}$C were considered unusually high for San Francisco. The $\geq 30\,^{\circ}$C threshold was selected because 29.72 °C is the Tukey upper inner fence for maximum daily air temperatures during the months with a risk probability greater than zero, April through July. It was necessary to use a statistical method for determining outliers such as the Tukey upper inner fence in order to determine an unbiased threshold for unusually high temperatures. The Tukey upper inner fence was calculated as one and one-half times the interquartile range above the upper quartile (Wilks, 2006). Statistics and graphs were completed in R (http://www.r-project.org), and the maps were made using the Generic Mapping Tool, GMT (Wessel & Smith, 1991). Risky months vary by geographic locations (Helmuth, 2002). Therefore, maps show the percentage of risky days in June because it is a risky month for all geographic locations shown in the map. In addition, June is a good month for risk observations because solar elevations reach their peak during the northern hemisphere summer solstice which makes it a particularly interesting time of year to observe the timing of low tide.

Results

The percentages of risky days in June are spatially and temporally variable along the West Coast of North America (Fig. 1). In terms of spatial variation, Oregon (OR) has a much higher percentage of risky days at mid shore level in June than Central and Southern California (CA). The result indicates, that in the absence of mitigating factors like coastal fog or clouds, risk of thermal extremes in June is higher in OR at this shore level than elsewhere on the US west coast. Decadal variation in the proportion of risky days, the main focus of this study, varied over the period 1980–2019 from 0% to >30% of

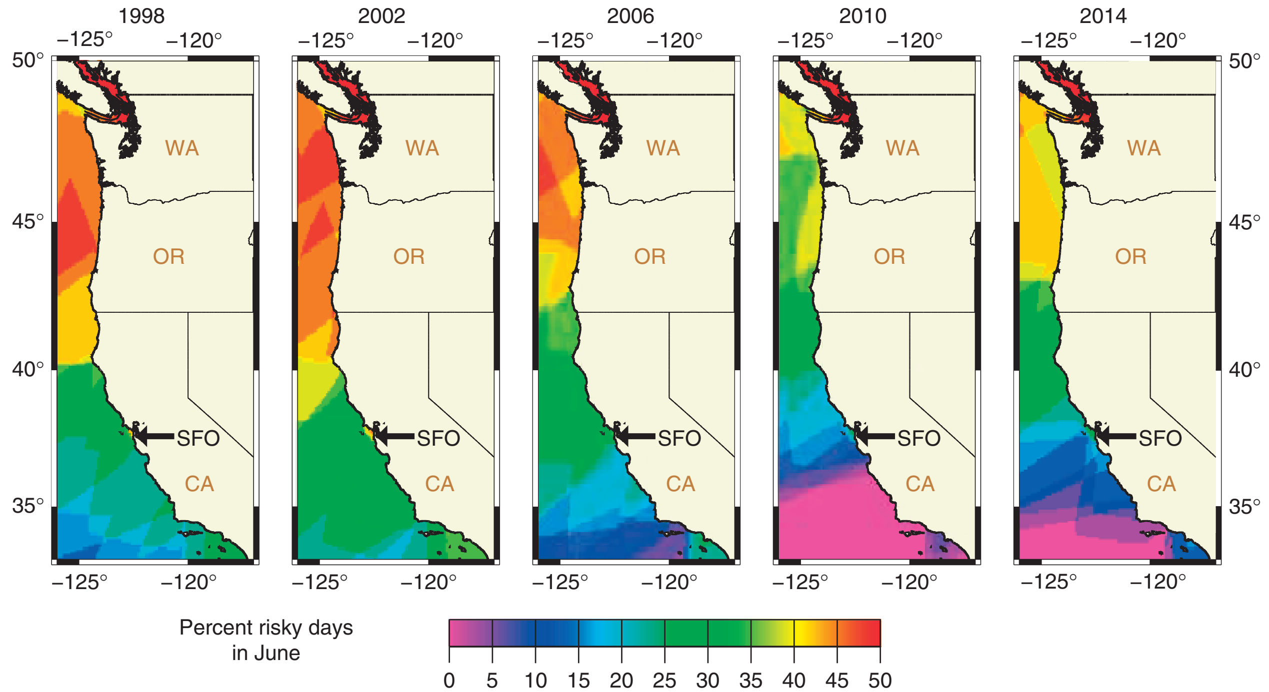

Fig. 1 Maps showing spatial and temporal variation in the intertidal risk probability (tidal effects) in June along the West Coast of North America. The June risk analysis was conducted for the years 1980 through 2019, although only 5 years are depicted here. These 5 years were selected to represent variation in risk during the 18.6-year tidal epoch with the 2002 map depicting a higher risk year and the 2010 map depicting a lower risk year. Risk is only relevant for intertidal areas at the land-sea interface but is shown over large areas of ocean for visualization purposes. The arrow labeled 'SFO' indicates the location of San Francisco, California. Abbreviations for the States are 'WA', Washington; 'OR', Oregon; and 'CA', California.

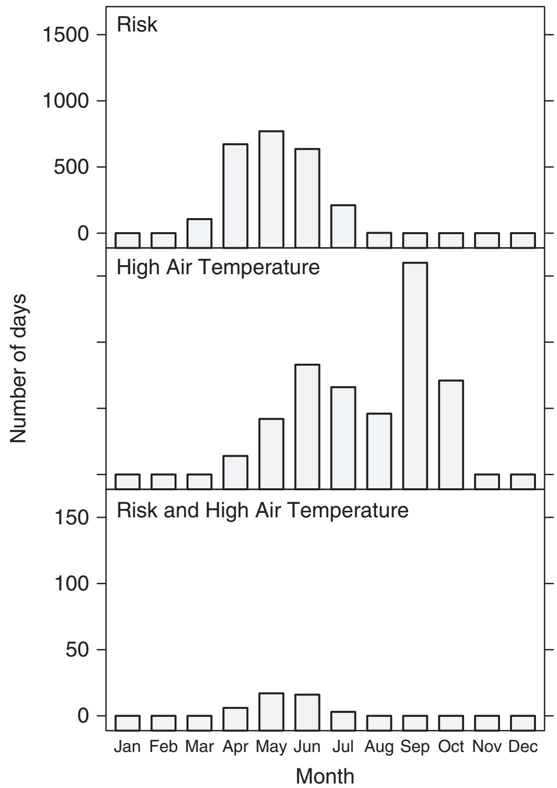

Fig. 2 A summary of the monthly variation in frequency of risk and frequency of air temperatures $\geq 30\,^{\circ}$C from 1950 through 2006 in San Francisco, California. The top graph, labeled 'Risk', has a different scale on the *y*-axis.

days in June at a single location, as is the case in Central and Southern California (Fig. 1). The year 2009, represents a time of lower risk probability along the West Coast of North America. Risk probability will not dramatically increase again in June until 2015, which will then be followed by several years of higher risk probability. This variation is caused by the 18.6-year lunar declination cycle (Brown *et al*., 2005).

In San Francisco, a monthly summary using data from 1950 until 2006 shows an overlap between risk and frequency of high air temperature, but the peaks are not synchronized (Fig. 2). The decoupling of risk and air temperature is presumably related to the seasonality of coastal clouds and fog as well as the seasonal variation in the timing of the lowest tides. The highest risk probability is in May while greatest frequency of high air temperatures, $\geq 30\,^{\circ}$C, is in September. May, the highest risk probability month, also has a relatively high frequency of high temperature days. Conversely, there is no risk in September, the month with the greatest number of high air temperature days because aerial exposure during times of high temperature is negligible. Annually, there is risk in the months of March through July, and there are high air temperatures in the months of April through October. Thus, there are only 4 months, April through July, with both risk of aerial exposure when the sun is high in the sky and when air temperatures are high.

In order to analyze the interactive effects of tidal risk and exposure to extreme air temperatures on an annual basis, data from April through July, 122 days, were combined and several probability statistics were calculated. Annual frequency of risky days ranged from a maximum value of 41% to a minimum value of 28% risky days. There is a 2.9% $\pm$ 2.1 ($\pm$ SD) chance a given day in the months April through July will be $\geq 30\,^{\circ}$C in San Francisco. The intertidal zone will be likely to experience high air temperatures on 1.24 $\pm$ 0.13 ($\pm$ SD) days per year based on the joint probability of risky days and hot days. Since there is typically one risky, high air temperature day per year in San Francisco, we only considered a year to be unusual if it contained greater than one risky, high air temperature day. There were nine unusual years between 1950 and the end of 2006 based on the parameters selected for this study. Fig. 3a shows that most of the unusual years tended to be years with a greater percentage of risky days. One time, 1973, in over 50 years, high air temperatures occurred on risky days in a year with a low percentage of risky days. However, 1973 was an unusual year because the number of high air temperature days was >1 SD above the annual mean (Fig. 3b). The greatest number of high air temperature days occurred in 1976. However, 1976 was a year with fewer risky days, 30%, and there were no risky, high temperature days. The record number of hot, risky days for a single year is 5 and occurred in 1985. Since oceanic conditions can influence coastal climates, we tested whether there was a correlation between risk and high air temperatures. There was no significant correlation between risk and high air temperatures ($P = 0.7591$, df $= 55$, $F = 0.09496$), which means that it was possible to treat risk and high air temperature as independent probabilities as we did in this analysis.

The ultimate goal of this modeling approach is to use risk to help determine future impacts of weather and climate on the intertidal ecosystem. In San Francisco, the percentage of risky days will reach the next low point in 2012. Then, the percentage of risky days will increase until 2019, the final year assessed by this study. 2015 has the potential to be an important year because it has 33% risky days, the historical threshold for an unusual number of risky, high temperature days (Fig. 3a).

Discussion

Hindcasts reveal that the timing of the tides has provided a theoretical measure of protection for intertidal organisms living on the outer coast near San Francisco

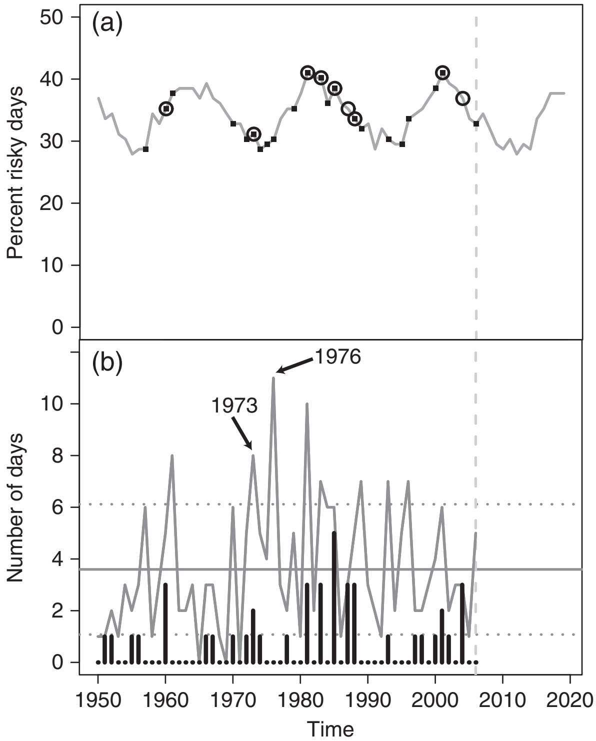

Fig. 3 A long-term synthesis of risk and air temperature $\geq$30 °C in the months April through July in San Francisco, California. In both graphs, the dotted vertical line represents 2006, the final year of air temperature data in this study. (a) Risk probability for 1950 through 2019. The overlaying squares and open circles indicate, respectively, the above average occurrence of air temperatures $\geq$30 °C and the above average occurrence of air temperatures $\geq$30 °C on risky days. (b) Frequency of air temperatures $\geq$30 °C (grey line) and frequency of air temperatures $\geq$30 °C on risky days (black bars). The solid grey horizontal line indicates the mean number of days $\geq$30 °C. The dotted grey horizontal lines indicate the SD for the mean number of days $\geq$30 °C.

from weather conditions associated with high air temperatures. This protection is evident on both monthly and decadal time scales. At the monthly scale, the disjunction between the months with the greatest frequency of risky days, May and June, and the month with the greatest frequency of $\geq$30 °C days means that there are few risky, hot days in the intertidal zone in San Francisco. Annual risk follows a decadal oscillation pattern of several higher risk years followed by several lower risk years that is related to changes in lunar declination (Denny & Paine, 1998; Helmuth *et al.*, 2002). During the time period, 1950 through 2006, there were three peaks in risk frequency: 1966, 1981, and 2001. These peaks in risk frequency in San Francisco roughly corresponded with the midpoints of the lunar declination cycle in 1964, 1982, and 2001, as the angle moved from its minimum to maximum value (Giorgini *et al.*, 1996). The next time the lunar declination reaches this point is in 2020. The 1980s time period had the most risky, hot days because it also had more hot days (April–July) than the other high risk time periods. In addition, increased frequencies of hot temperatures led to more risky, hot days in a year with low risk, 1973. Climatological analysis, as used here, reveals historical trends in weather conditions experienced by the intertidal ecosystem so that unusual events can be identified in the future.

The patterns of risk and air temperatures in San Francisco are related to the general tidal and climatic characteristics of the West Coast of North America. The tides along the West Coast of North America are mixed semi-diurnal which means that there are two high tides and two low tides per day but the magnitude of one high tide is larger than the other high tide and the magnitude one low tide is smaller than the other low tide (Brown *et al.*, 2005). The riskiest time period for exposure to adverse weather conditions for animals living near the midpoint of the tidal range is during the lowest tide which occurs approximately once per day. The timing of the lowest tide shifts over the 18.6-year tidal epoch creating the variation in risk seen in Fig. 1 between years. In contrast, coastlines with semi-diurnal tides, including Europe and the East Coast of North America, have two high tides and two low tides of equal magnitude per day which means that shifts in the timing of the low tides over the 18.6-year tidal epoch do not cause as much annual variation in risk. In other words, as one low tide shifts to later in the day, the other low tide shifts to the middle of the day resulting in smaller differences in risk probability between years (unpublished data). In addition, it is important to emphasize that the focus of this study is the midpoint of the tidal range and risk will change depending on the shore level of the organism. There will be more frequent risk for organisms living at shore levels above the midpoint and reduced risk for organisms living at shore levels below the midpoint. The progression of change in risk at shore levels above the midpoint of the tidal range is an important area of future research.

The climate near San Francisco is shaped by the geography of the region and patterns of coastal currents (Elford, 1974). One of the most dominant characteristics of the summer weather in San Francisco is the presence of fog. Northwest winds drive the California Coastal Current from north to south along the coast which causes upwelling of cold water from deeper ocean waters (Elford, 1974). Coastal fog forms as the warm, moist air from the Pacific passes over the cold, upwelled water and is pushed toward land by the northwest winds (Elford, 1974). Fog keeps the temperatures cool along the San Francisco coastline which is the main reason the frequency of $\geq 30\,^{\circ}C$ days is greater in September than in any of the summer months. In the absence of fog, there would be many more $\geq 30\,^{\circ}C$ days during the summer since the high pressure over the Pacific deflects storms causing the air mass above the fog to be clear and cloudless for most of the summer (Elford, 1974). Therefore, in addition to tides and solar elevation, fog also decreases exposure to weather conditions that lead to high temperatures for intertidal organisms.

The Pacific Decadal Oscillation (PDO) and El Niño also influence the marine intertidal region with cyclic periodicities of warmer and cooler ocean temperatures of 20–30 years and 2–7 years, respectively (Bridgman & Oliver, 2006; Rohli & Vega, 2008). However, there does not appear to be a direct connection between the frequency of $\geq 30\,^{\circ}C$ air temperature days or risky days and either of these oceanic fluctuations despite their influence on the regional climate. There are two clusters, 1970–1976 and 1981–1985, of above normal frequencies of $\geq 30\,^{\circ}C$ days (Fig. 3a). The 1970–1976 cluster of $\geq 30\,^{\circ}C$ days occurred during the cool phase of the PDO and included only weak 'El Niño-like' conditions. It also occurred during a period of reduced annual risk so there was only one year with an above average number of hot, risky days. However, the cluster of $\geq 30\,^{\circ}C$ days between 1981 and 1985 is consistent with the warm phase of the PDO and includes the strong 1982–1984 El Niño event (Mantua *et al.*, 1997; Mantua & Hare, 2002; Bridgman & Oliver, 2006). The 1981–1985 cluster was during a period of higher relative risk and included 3 years with above average numbers of risky, hot days for the marine intertidal zone (Fig. 3a). The frequencies of $\geq 30\,^{\circ}C$ were only calculated for the risky months, April through July, which may explain the lack of a connection with the oceanic oscillations which can vary seasonally (Chiba *et al.*, 2006). The time period 1981–1985 is particularly notable because of the high frequencies of risky, hot days, and above average ocean temperatures during the El Niño which means that marine intertidal organisms were experiencing above normal temperature conditions during both low and high tide. Changes in intertidal ecosystems were observed following this time period and are believed to be related to environmental stress (Dayton & Tegner, 1990; Raimondi *et al.*, 2002).

No biological data were used in this analysis so it is impossible to determine specific impacts, if any, of air temperatures $\geq 30\,^{\circ}C$ (Kearney, 2006). Organism body temperature, determined by a suite of factors, is the ultimate driver of temperature-related physiological stress and mortality (Porter & Gates, 1969; Helmuth, 2002). External determinants of body temperature include air temperature, but other factors such as solar radiation, organism morphology, and microsite are also important (Helmuth, 1998). These factors must be considered before the consequences of risky, hot days can be determined quantitatively for individual intertidal organisms. The recent increase in the availability of weather records can be matched to this type of risk analysis to help evaluate some of the consequences of high air temperature weather conditions. For example, Harley (2008) observed increased mussel mortality at Bodega Bay, which is located just north of San Francisco, following the unusual number of risky, $\geq 30\,^{\circ}C$ days in 2004 (Fig. 3). The risk analysis, in return, can provide scientists with advance notice of when to be prepared to observe heat-related mortality events in the marine intertidal zone (Hannah *et al.*, 2002).

There are several points to consider when deciding whether to employ the intertidal risk analysis. A major advantage to this analysis is that it can be applied on a worldwide basis. The OTIS tide models are available for all regions of the world because they include satellite measurements. Air temperature is a commonly available weather parameter collected as part of long-term datasets which is why it was chosen as a proxy for evaluating weather conditions. Thus, this is meant to be a broadly applicable method. However, there are likely to be locations where the intertidal risk analysis will require modification. The tide elevations generated by models are predictions. Real tides deviate from tidal predictions depending on wind, waves, and air pressure. In particular, wave surge and wave splash can blur tidal movement (Porter & Gates, 1969; Harley & Helmuth, 2003). Air temperature is an effective proxy for summer weather conditions in San Francisco because the climate is dominated by the Pacific Ocean – foggy days have cooler air temperatures, and sunny days have warmer temperatures (Elford, 1974). Solar radiation is one of the major factors driving intertidal organism body temperature making the relationship between air temperature and sunshine in San Francisco meaningful (Porter & Gates, 1969; Helmuth, 1998, 1999; Wethey, 2002; Gilman *et al.*, 2006b). Therefore, solar radiation should also be considered if data are available.

In summary, risk analyses of nonclimatic factors serve as an effective means of generating broad scale hypotheses that can then be tested in the field. They can provide first order estimates of how mortality might change over time, and are critical for addressing how local, nonclimatic factors may overwhelm the effects of large-scale gradients in climate. In order to adapt the approach presented to specific organisms, additional site- and species-specific modifications are needed (Gilman *et al.*, 2006b). Such approaches will become increasingly important in the face of climate change, as results of these simulations suggest that nonclimatic factors can play a significant role in modifying the observed effects of climate change on intertidal communities.

Acknowledgements

We thank Kyle Aveni-Deforge, James Hench, and Joshua Cooper for assistance and advice at various stages of this project. This manuscript was greatly improved by comments from V. Lakshmi, S. Woodin, and three anonymous reviewers. This research was supported by a NASA Earth Systems Science Fellowship, NASA Grant NNG04GE43G, and NOAA Ecofore Grant NA04-NOS4780264.

References

Araújo MB, Pearson RG, Thuiller W, Erhard M (2005) Validation of species-climate impact models under climate change. *Global Change Biology*, **11**, 1504–1513.

Bell EC (1995) Environmental and morphological influences on thallus temperature of the intertidal alga *Mastocarpus papillatus* Kützing. *Journal of Experimental Marine Biology and Ecology*, **191**, 29–55.

Blanchette CA, Miner CM, Raimondi PA, Lohse D, Heady KEK, Broitman BR (2008) Biogeographic patterns of rocky intertidal communities along the Pacific coast of North America. *Journal of Biogeography*, **35**, 1593–1607.

Bonan GB (2002) *Ecological Climatology*. Cambridge University Press, Cambridge, UK.

Bridgman HA, Oliver JE (2006) *The Global Climate System*. Cambridge University Press, New York.

Broitman BR, Blanchette CA, Menge BA *et al*. (2008) Spatial and temporal patterns of intertidal invertebrate recruitment along the West coast of the United States. *Ecological Monographs*, **78**, 403–421.

Brown E, Colling A, Park D, Wright J (2005) *Waves, Tides and Shallow-Water Processes*. Butterworth-Heinemann, Oxford.

Burnaford JL, Vasquez M (2008) Solar radiation plays a role in habitat selection by the sea star *Pisaster ochraceous*. *Marine Ecology Progress Series*, **368**, 177–187.

Burrows MT, Hughes RN (1989) Natural foraging of the Dog-whelk, *Nucella lapillus* (Linnaeus); The weather and whether to feed. *Journal of Molluscan Studies*, **55**, 285–295.

Chiba S, Tadokoro K, Sugisaki H, Saino T (2006) Effects of decadal climate change on zooplankton over the last 50 years in the western subarctic North Pacific. *Global Change Biology*, **12**, 907–920.

Darlington PJ (1957) *Zoogeography: The Geographical Distribution of Animals*. Harvard University Press, Cambridge, MA.

Davies AJ, Johnson MP (2006) Coastline configuration disrupts the effects of large-scale climatic forcing, leading to divergent temporal trends in wave exposure. *Estuarine, Coastal, and Shelf Science*, **69**, 642–648.

Davis AJ, Jenkinson LS, Lawton JH, Shorrocks B, Wood S (1998) Making mistakes when predicting shifts in species range in response to global warming. *Nature*, **391**, 783–786.

Dayton PK, Tegner MJ (1990) Bottoms beneath troubled waters: Benthic impacts of the 1982–1984 El Niño in the temperate zone. In: *Global Ecological Consequences of the 1982–83 El Niño-Southern Oscillation*. (ed. Glynn PW) pp. 433–472. Elsevier, Amsterdam.

Denny MW, Harley CDG (2006) Hot limpets: predicting body temperature in a conductance-mediated thermal system. *The Journal of Experimental Biology*, **209**, 2409–2419.

Denny MW, Miller LP, Harley CDG (2006) Thermal stress on intertidal limpets: long-term hindcasts and lethal limits. *The Journal of Experimental Biology*, **209**, 2420–2431.

Denny MW, Paine RT (1998) Celestial mechanics, sea-level changes, and intertidal ecology. *Biological Bulletin*, **194**, 108–115.

Easterling DR, Meehl GA, Parmesan C, Changnon SA, Karl TR, Mearns LO (2000) Climate extremes: observations, modeling, and impacts. *Science*, **289**, 2068–2074.

Egbert G, Bennett A, Foreman M (1994) TOPEX/Poseidon tides estimated using a global inverse model. *Journal of Geophysical Research*, **99**, 24821–24852.

Egbert G, Erofeeva S (2002) Efficient inverse modeling of barotropic ocean tides. *Journal of Atmospheric and Oceanic Technology*, **19**, 183–204.

Elford CR (1974) *The Climate of California. Climates of the States*. Water Information Center Inc., Port Washington pp. 538–594.

Etter RJ (1998) Physiological stress and color polymorphism in the intertidal snail *Nucella lapillus*. *Evolution*, **42**, 660–680.

Finke GR, Navarette SA, Bozinovic F (2007) Tidal regimes of temperate coasts and their influences on aerial exposure for intertidal organisms. *Marine Ecology Progress Series*, **343**, 57–62.

Franco AMA, Hill JK, Kitschke C *et al*. (2006) Impacts of climate warming and habitat loss on extinctions at species' low-latitude range boundaries. *Global Change Biology*, **12**, 1545–1553.

Gilman SE, Harley CDG, Strickland D, Vanderstraeten O, O'Donnell M, Helmuth B (2006a) Evaluation of ''Effective Shore Level'' as a method of characterizing intertidal wave exposure regimes. *Limnology and Oceanography: Methods*, **4**, 448–457.

Gilman SE, Wethey DS, Helmuth B (2006b) Variation in the sensitivity of organismal body temperature to climate change over local and geographic scales. *Proceedings of the National Academy of Sciences*, **103**, 9560–9565.

Giorgini JD, Yeomans DK, Chamberlin AB *et al*. (1996) JPL's on-line solar system data service. *Bulletin of the American Astronomical Society*, **28**, 1158.

Hannah L, Midgley GF, Millar D (2002) Climate change-integrated conservation strategies. *Global Ecology and Biogeography*, **11**, 485–495.

Harley CDG (2008) Tidal dynamics, topographic orientation, and temperature-mediated mass mortalities on rocky shores. *Marine Ecology Progress Series*, **371**, 37–46.

Harley CDG, Helmuth B (2003) Local- and regional-scale effects of wave exposure, thermal stress, and absolute versus effective shore level on patterns of intertidal zonation. *Limnology and Oceanography*, **48**, 1498–1508.

Helmuth B (1998) Intertidal mussel microclimates: predicting the body temperature of a sessile marine invertebrate. *Ecological Monographs*, **68**, 51–74.

Helmuth B (1999) Thermal biology of rocky intertidal mussels: quantifying body temperatures using climatological data. *Ecology*, **80**, 15–34.

Helmuth B (2002) How do we measure the environment? Linking intertidal thermal physiology and ecology through biophysics. *Integrative and Comparative Biology*, **42**, 837–845.

Helmuth B, Broitman BR, Blanchette CA *et al*. (2006a) Mosaic patterns of thermal stress in the rocky intertidal zone: implications for climate change. *Ecological Monographs*, **76**, 461–479.

Helmuth B, Harley CDG, Halpin PM, O'Donnell M, Hofmann GE, Blanchette CA (2002) Climate change and latitudinal patterns of intertidal thermal stress. *Science*, **298**, 1015–1017.

Helmuth B, Mieszkowska N, Moore P, Hawkins SJ (2006b) Living on the edge of two changing worlds: forecasting the responses of rocky intertidal ecosystems to climate change. *Annual Review of Ecology, Evolution, and Systematics*, **37**, 373–404.

Holtmeier F-K, Broll G (2005) Sensitivity and response of northern hemisphere altitudinal and polar treelines to environmental change at landscape and local scales. *Global Ecology and Biogeography*, **14**, 395–410.

Hsieh CH, Reiss CS, Hewitt RP, Sugihara G (2008) Spatial analysis shows that fishing enhances the climatic sensitivity of marine fishes. *Canadian Journal of Fisheries and Aquatic Sciences*, **65**, 947–961.

Huey RB, Peterson CR, Arnold SJ, Porter WP (1989) Hot rocks and not-so-hot rocks: retreat-site selection by garter snakes and its thermal consequences. *Ecology*, **70**, 931–944.

Hutchins LW (1947) The bases for temperature zonation in geographical distribution. *Ecological Monographs*, **17**, 325–335.

IPCC (2007) *Climate change 2007: synthesis report*. Contribution of Working Groups I, II, and III to the Fourth Assessment Report of the Intergovernmental Panel on Climate Change. (eds. Core Writing Team, Pachauri RK, Reisinger A), Geneva, Switzerland, 104 pp.

Kearney M (2006) Habitat, environment and niche: what are we modelling? *Oikos*, **115**, 186–191.

Kenyon J, Hegerl GC (2008) Influence of modes of climate variability on global temperature extremes. *Journal of Climate*, **21**, 3872–3888.

Körner C (1998) A re-assessment of high elevation treeline positions and their explanation. *Oecologia*, **115**, 445–459.

Lewis JR (1964) *The Ecology of Rocky Shores*. English Universities Press, London.

Light SF, Smith FI, Pitelka FA, Abbott DP, Wesner FM (1954) *Intertidal Invertebrates of the Central California Coast*. University of California Press, Berkeley.

Lima FP, Queiroz N, Ribeiro PA, Hawkins SJ, Santos AM (2006) Recent changes in the distribution of a marine gastropod, *Patella rustica* Linnaeus, 1758, and their relationship to unusual climatic events. *Journal of Biogeography*, **33**, 812–822.

Lima FP, Ribeiro PA, Queiroz N, Hawkins SJ, Santos AM (2007) Do distributional shifts of northern and southern species of algae match the warming pattern? *Global Change Biology*, **13**, 2592–2604.

MacArthur RH (1972) *Species Distributions. Geographical Ecology.* Harper & Row, New York, 127–168 pp.

Mantua NJ, Hare SR (2002) The Pacific Decadal Oscillation. *Journal of Oceanography*, **58**, 35–44.

Mantua NJ, Hare SR, Zhang Y, Wallace JM, Francis RC (1997) A Pacific interdecadal climate oscillation with impacts on salmon production. *Bulletin of the American Meteorological Society*, **78**, 1069–1079.

Moore P, Hawkins SJ, Thompson RC (2007) Role of biological habitat amelioration in altering the relative responses of congeneric species to climate change. *Marine Ecology Progress Series*, **334**, 11–19.

Morin XA, Augspurger C, Chuine I (2007) Process-based modeling of species' distributions: what limits temperate tree species' range boundaries. *Ecology*, **88**, 2280–2291.

Morin XA, Viner D, Chuine I (2008) Tree species range shifts at a continental scale: new predictive insights from a processed-based model. *Journal of Ecology*, **96**, 784–794.

Moritz C, Patton JL, Conroy CJ, Parra JL, White GC, Beissinger SR (2008) Impact of a century of climate change on small-mammal communities in Yosemite National Park USA. *Science*, **322**, 261–264.

Parmesan C (2006) Ecological and evolutionary responses to recent climate change. *Annual Review of Ecology, Evolution, and Systematics*, **37**, 637–669.

Pearson RG, Dawson TP (2003) Predicting the impacts of climate change on the distribution of species: are bioclimate envelope models useful? *Global Ecology and Biogeography*, **12**, 361–371.

Pearson RG, Thuiller W, Araújo MB *et al*. (2006) Model-based uncertainty in species range prediction. *Journal of Biogeography*, **33**, 1704–1711.

Poloczanska ES, Hawkins SJ, Southward AJ, Burrows MT (2008) Modeling the response of populations of competing species to climate change. *Ecology*, **89**, 3138–3149.

Porter WP, Gates D (1969) Thermodynamic equilibria of animals with environment. *Ecological Monographs*, **39**, 245–270.

Porter WP, Sabo JL, Tracy CR, Reichman OJ, Ramankutty N (2002) Physiology on a landscape scale: plant-animal interactions. *Integrative and Comparative Biology*, **42**, 431–453.

Raimondi PA, Wilson CM, Ambrose RF, Engle JM, Minchinton TE (2002) Continued declines of black abalone along the coast of California: are mass mortalities related to El Niño events? *Marine Ecology Progress Series*, **242**, 143–152.

Ricketts EF, Calvin J (1939) *Between Pacific Tides*. Stanford University Press, Palo Alto.

Robinson IS (2004) *Measuring the Oceans from Space*. Springer - Praxis, Berlin.

Rohli RV, Vega AJ (2008) *Climatology.* Jones and Bartlett Publishers, Boston.

Sala OE, Chapin FS, Armesto JJ *et al*. (2000) Biodiversity – Global biodiversity scenarios for the year 2100. *Science*, **287**, 1770–1774.

Schoch GC, Menge BA, Allison G, Kavanaugh M, Thompson SA, Wood SA (2006) Fifteen degrees of separation: latitudinal gradients of rocky intertidal biota along the California Current. *Limnology and Oceanography*, **51**, 2564–2585.

Southward AJ (1958) Note on the temperature tolerances of some intertidal animals in relation to environmental temperatures and geographical distribution. *Journal of Marine Biological Association of the United Kingdom*, **37**, 49–66.

Sutherst RW, Maywald GF, Bourne AS (2007) Including species interactions in risk assessments for global change. *Global Change Biology*, **13**, 1843–1859.

Szathmary PL, Helmuth B, Wethey DS (2009) Climate change in the rocky intertidal zone: predicting and measuring the body temperature of an intertidal keystone predator. *Marine Ecology Progress Series*, **374**, 43–56.

Thuiller W (2003) BIOMOD – optimizing predictions of species distributions and projecting potential future shifts under global change. *Global Change Biology*, **9**, 1353–1362.

Wessel P, Smith WHF (1991) Free software helps map and display data. *EOS Transactions of the American Geophysical Union*, **72**, 441, 445–446.

Wethey DS (1985) Catastrophe, extinction, and species diversity: a rocky intertidal example. *Ecology*, **66**, 445–456.

Wethey DS (1986) Climate and biogeography: continuous versus catastrophic effects on rocky intertidal communities. *Estudios Oceanológicos*, **5**, 19–25.

Wethey DS (2002) Biogeography, competition, and microclimate: the barnacle *Chthamalus fragilis* in New England. *Integrative and Comparative Biology*, **42**, 872–880.

Wethey DS, Woodin SA (2008) Ecological hindcasting of biogeographic responses to climate change in the European intertidal zone. *Hydrobiologia*, **606**, 139–151.

Wilks DS (2006) *Statistical Methods in the Atmospheric Sciences*. Academic Press, Boston.